



Disparity and Evolutionary Rate Do Not Explain Diversity Patterns in Muroid Rodents (Rodentia: Muroidea)

Bader H. Alhajeri¹ · Scott J. Steppan²

Received: 22 January 2018 / Accepted: 25 April 2018 / Published online: 28 April 2018
© Springer Science+Business Media, LLC, part of Springer Nature 2018

Abstract

A positive correlation between diversity and disparity/evolutionary rate is predicted by multiple evolutionary theories. However, recent empirical studies in various taxa do not always find such an association. Similarly, we find no correlation between these two levels of variation, based on cranial morphometric data and molecular phylogenetic data from 317 muroid rodent species and dipodoid outgroups, analyzed using three-dimensional geometric morphometrics. This disassociation was found using both phylogenetic and non-phylogenetic approaches, indicating that an increase in clade richness is not necessarily followed by an increase in morphological divergence and vice versa. Furthermore, the distribution of muroid families in morphospace is highly overlapping suggesting greater variation within than between clades. Taken together with the observation that families with the most distinctive cranial morphologies (nesomyids, dipodids, and spalacids) are the least diverse, indicates that evolution of new cranial morphologies may not play an important role in the diversification of muroid rodents.

Keywords Clade richness · Crania · Diversification · Geometric morphometrics · Morphological divergence · Phylogeny

Introduction

Clade variation is the amount of taxonomic diversity (number of species or genera) and phenotypic disparity (how distinct clade members are from one another; Foote 1993). Both diversity and disparity are closely associated with ecological divergence. Muroid rodents are the most diverse superfamily of mammals, comprising >28% of all mammal species (Musser and Carleton 2005). Muroids are also among the most variable in ecological attributes including locomotion, diet, and behavior (Nowak 1999). The diversity of muroid rodents is often explained as arising from multiple independent adaptive radiations (Patterson and Pascual 1968).

Recent work has shown that muroids have undergone frequent diversification shifts in various clades (24 in the Myodonta, Fabre et al. 2012; 28 in Muroidea; Schenk et al. 2013). However, the main cause of uneven diversification patterns in muroids remains elusive. Shifts in muroid diversification rates (rates at which new species form) are not satisfactorily explained by ecological opportunity mediated by biogeographic transitions (Schenk et al. 2013; Alhajeri et al. 2016) nor by trait evolution (diet, habitat, body mass, and relative tail length, Alhajeri and Steppan 2018). In both Alhajeri et al. (2016) and Alhajeri and Steppan (2018), the association between diversity and disparity/evolutionary rate is implied but not directly tested. We explicitly examine this association in the present study, by testing the correlation between diversity indices (log richness and diversification rate) with disparity and evolutionary rate.

One of the earliest evolutionary theories that predict a positive relationship between diversity and disparity/evolutionary rate is Gould and Eldredge's (1977) punctuated equilibrium hypothesis, which postulates that most phenotypic divergence occurs at speciation events, which are followed by long periods of stasis until the next speciation event. Consequently, clade diversification rate is expected to be correlated with its phenotypic divergence (Ricklefs 2004, 2006). This relationship is also predicted by the theory of

Electronic supplementary material The online version of this article (<https://doi.org/10.1007/s11692-018-9453-z>) contains supplementary material, which is available to authorized users.

✉ Bader H. Alhajeri
bader.alhajeri@ku.edu.kw

¹ Department of Biological Sciences, Kuwait University, 13110 Safat, Kuwait

² Department of Biological Science, Florida State University, Tallahassee, FL 32306-4295, USA

ecological adaptive radiation (*sensu* Schluter 2000) whereby lineages that exploit ecological opportunities undergo an early increase in phylogenetic diversification, which occurs in concert with functional, adaptive, and phenotypic divergence as recently diverged species occupy new ecological niches. This early increase in diversification is followed by a density dependent decline in both the rate of diversification and divergence associated with the crowding of adaptive zones (Simpson 1944; Freckleton and Harvey 2006).

These theories assume that phenotypic and ecological divergence are positively correlated with reproductive isolation, a pattern that is supported in plant, invertebrate, and vertebrate taxa (Funk et al. 2006). However, diversification can occur without phenotypic/ecological divergence, at least initially, through geographic isolation and “non-adaptive radiation,” that leads to ecologically similar species that diverge in sympatry; a pattern that is associated with recent radiations, as subsequent divergence in old radiations renders their pattern indistinguishable from adaptive radiations (Rundell and Price 2009).

Ricklefs (2004) was one of the earliest to test the correlation between phenotypic disparity and species diversity and found the association to be significant in passerine birds. This correlation was later attributed to variation in clade age—not to the rates of diversification and phenotypic evolution (Purvis 2004; Ricklefs 2006). Adams et al. (2009) did not find a significant correlation between diversification rates and phenotypic evolution rates of both body size and shape in 190 species of plethodontid salamanders, which they interpreted as due to rapid diversification with little morphological change or to rapid morphological evolution with little speciation. Later, they tested the correlation between morphological and ecological variation (microhabitat use) and found that morphology is not a good index of ecology in their examined group, as they are largely decoupled (Blankers et al. 2012). Interestingly, when they examined the correlation between the rates of morphological evolution (using the same body size and shape dataset) and log species richness (number of species in a clade), instead of species diversification rates, they did find a significant positive correlation, which is consistent with the hypothesis that increased morphological evolution rates promote diversification (Rabosky and Adams 2012). This discrepancy was interpreted as due to diversification not being modeled adequately as a simple time-dependent process in their system (Rabosky and Adams 2012).

Using phylogenetic generalized least squares (PGLS) multiple regression analyses (Martins and Hansen 1997), Gonzalez-Voyer et al. (2011) found that species richness and diversification rate were not significantly correlated with clade-age in a clade of *Terrarana* frogs. Instead, a combination of ecological and phenotypic traits (skin attributes, altitude, body size) explain most of the diversity variation,

a pattern that suggests a positive correlation between diversity and disparity/evolutionary rate in this group (Gonzalez-Voyer et al. 2011). Similarly, in a large sample of ray-finned fishes, Rabosky et al. (2013) found that rates of body size evolution are highly positively correlated with species diversification rates.

Although they did not directly test the correlation between diversity and disparity/evolutionary rate; by testing the predictions of adaptive radiation in a clade of 84 neocete cetaceans using node height tests (Freckleton and Harvey 2006) and disparity through time plots (Harmon et al. 2003), Slater et al. (2010) found that cetaceans underwent a significant increase in body size disparity with little increase in diversity. This pattern was explained as due to high extinctions, or fluctuations in diversification rates leading to the decoupling of these two variables, or that diversification and ecomorphological disparity are uncorrelated in this group (Slater et al. 2010). Similarly, Rowe et al. (2011) found that the recent radiation of the most diverse rodent genus, *Rattus*, consisting of 66 species and among the highest reported rates of diversification in vertebrates, was not associated with a significant increase in phenotypic disparity (based on twenty morphological measurements and two ecological characters), an expected result, given that this genus lacks overt ecomorphological variation. High diversity with low disparity (i.e. “non-adaptive radiation,” Rundell and Price 2009) is common in young clades, whereas the opposite pattern is more common in old clades and is precipitated by the cumulative effect of extinction at the late history of a clade, rather than increased rates of phenotypic evolution (Hopkins 2013).

The mammalian studies suggest that diversification is generally not correlated with morphological divergence in this group, in either old or recent radiations. However, diversification was not explicitly measured in Slater et al. (2010) and was unexceptional a priori, whereas the group chosen by Rowe et al. (2011) did not show sufficient external ecomorphological variation to robustly test for disparity/evolutionary rate. This, together with the relatively small species sample sizes make these studies suboptimal in testing the correlation between diversity and disparity/evolutionary rate in mammals.

In the present study, the correlation between diversity indices and disparity/evolutionary rate are directly tested in muroid rodent clades, a group that is optimal to test this question given the extent of variation in both these indices. The present study has numerous advantages, including the use of the newly estimated molecular phylogeny of the group (Schenk et al. 2013; Steppan and Schenk 2017), the relatively large sample size of clades, the use of both size and shape morphological datasets to quantify disparity/evolutionary rate, the use of both phylogenetic and non-phylogenetic estimates of diversity, and the use of alternative clade

designations. In addition, we quantify disparity/evolutionary rate in the cranium using three dimensional geometric morphometric (GM) approaches, which is not common in studies of association between diversity and disparity/evolutionary rate, where more common linear morphometric (LM) approaches are used. Because results from different approaches to quantify skull morphology may differ (e.g. a study of the mandible morphology of caviomorph rodents by Álvarez and Perez (2013) led to two different results when they quantified the mandibles in two dimensions vs. three dimensions) and because cranial morphology estimated using three dimensional landmark coordinate data is commonly converted into one dimensional distance measurements prior to analyses (e.g. Cheverud 1995; Marroig and Cheverud 2001; Wilson and Sánchez-Villagra 2010); we also quantify disparity/evolutionary rate using LM and compare the results with GM. Additional patterns examined in this study include the association between: (1) diversification rates and net diversity (log species richness); (2) morphological evolution rates and disparity; (3) clade age versus net diversity and disparity; and (4) shape versus size evolution and disparity.

Materials and Methods

Phylogenetic Sampling

Diversity indices were quantified from a 317-species chronogram extracted from Steppan and Schenk's (2017) 913 species tree of muroid rodents and dipodoid outgroups—the tree was based on multiple nuclear and mitochondrial markers and included multiple fossil calibrations. Nearly all species are found in the topologically congruent 297 species chronogram of Schenk et al. (2013). Species were sampled proportional to extant diversity and representative of the extent of morphological disparity; both species typical of clades and morphological outliers were chosen (subject to museum availability) to approximate dispersion of clades in morphospace. This resulted in the sampling of all extant subfamilies and 73% of muroid genera (Fig. 1; see the electronic supplementary material, Table S1). Four species lacking molecular data (*Lophuromys flavopunctatus*, *Gerbillus gleadowi*, *Gerbillus cheesmani*, and *Apodemus sylvaticus*) were grafted onto the tree as polytomies using the APE library (Paradis et al. 2004) in R (R Development Core Team 2017) based on taxonomic information from Musser and Carleton (2005) and are indicated by asterisks in Fig. 1.

Chronological Clade Sampling

Diversity indices and disparity/evolutionary rate were compared between non-nested clades. Clades were not based on

taxonomic rank (e.g. subfamily, genus) because these ranks originate at different ages. Rather, clade comparisons were conducted on a sample of origination times, on all clades present after the selected time for which at least three species appear in the morphological dataset. The number of suitable clades for comparison is maximized at 36 clades occurring at 5 mya and is reduced to 16 clades at 2.5 mya; although there are more clades at 2.5 mya, these have less than three species with morphological data. Clade comparisons were conducted at four origination times between 5 and 12.5 Mya (Table 1; Fig. 1). This was done because of the tradeoff between number of clades and accuracy of disparity estimates; young clades improve the power of the analyses due to the increase in sample size, but this comes at the expense of confidence in the disparity estimates, due to less of the variance being captured per clade. In addition, the phylogeny of younger clades is less well established (i.e. many subgenera are not monophyletic); therefore, the number of species (total diversity) in younger subclades is harder to determine than older clades because genera are split across multiple young clades. For this reason, the most recent age at which clades were compared is at 5 mya.

Diversity and Diversification Rate Estimates

Although many studies use diversification rates as a surrogate for clade diversity, this measure assumes that species number in clades increases unbounded through time; however, diversification rates are not always strongly correlated with species richness (Rabosky 2009a, b). Consequently, species richness may be a better estimate for clade diversity than diversification rates (Rabosky 2009a, b). In this study, we used both diversification rate and species richness. We used log total extant species richness, including unsampled species. Diversification rates were based on total extant species richness and clade age from the Steppan and Schenk (2017) muroid chronogram; calculated using the method-of-moments estimator for crown groups (Magallón and Sanderson 2001) using the GEIGER library (Harmon et al. 2008) in R.

Since extinction rates are unknown, we calculated diversification rates with no extinction (0.0), moderate extinction (0.5), and high extinction (0.9). The results were similar (data not shown) and we only present results using moderate relative extinction rate (0.5). For both diversity and diversification rate estimates, total species richness per clade was based on all known species, including species not sampled in the phylogeny, based on the taxonomy of Musser and Carleton (2005) with updates for newly described and unnamed species in Schenk et al. (2013) and Steppan and Schenk (2017). Log richness, diversification rates, and associated variables are indicated in Table 2 (see the electronic supplementary material, Table S2).

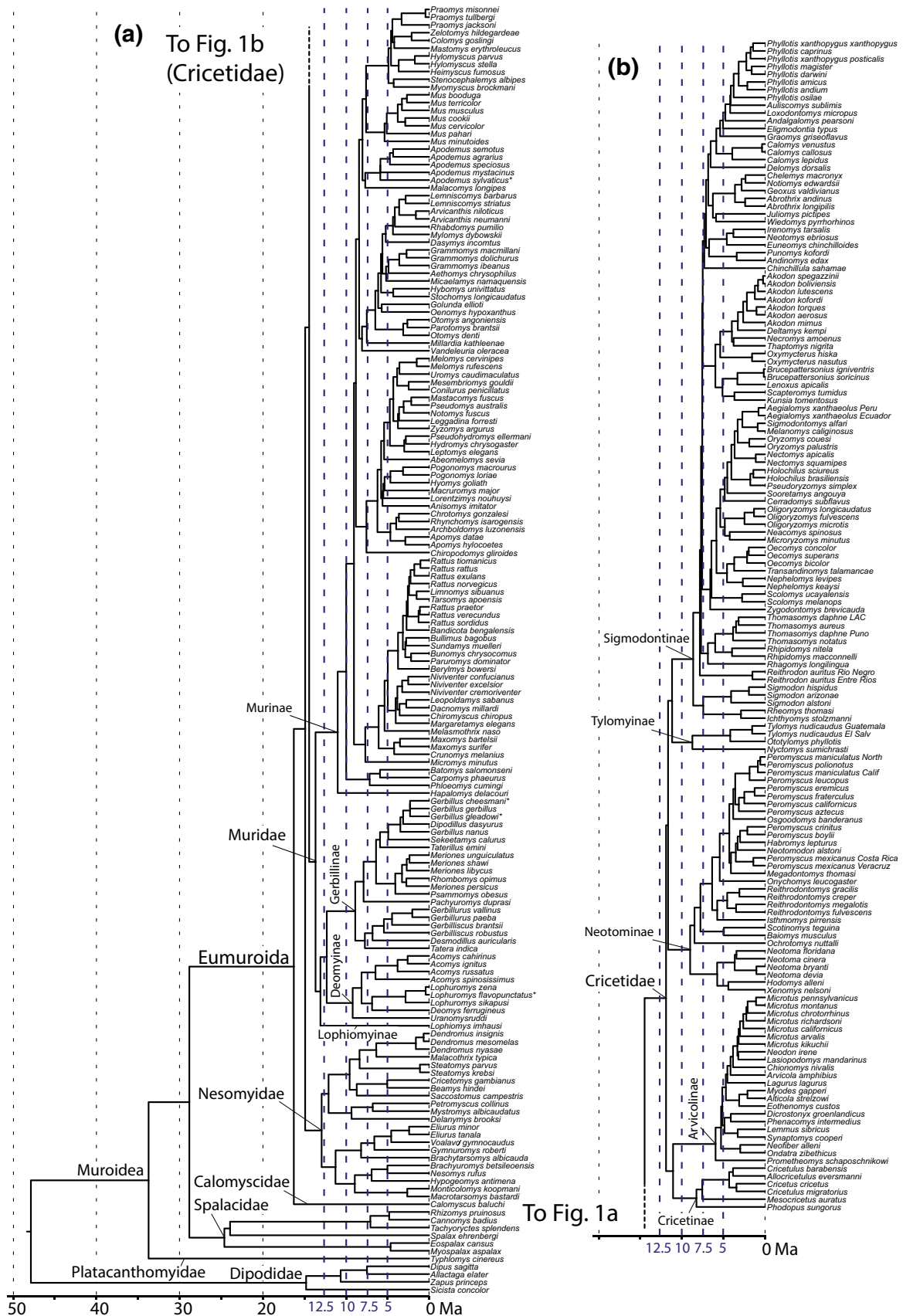


Fig. 1 Myodont rodent chronogram modified from the molecular phylogeny of Steppan and Schenk (2017). Most species are found in Schenk et al. (2013). Blue dashed lines indicate the four chronological sampling intervals. Some of the major taxonomic groups are indicated. (Color figure online)

Morphological Data Collection

A detailed description of the data collection and process is found in Alhajeri (2014) and will only be summarized here. We digitized one to six specimens per species (average = 4) to account for intraspecific variation and calculate species averages. Whenever possible, we sampled equal numbers of males and females of each species to account for sexual dimorphism, which is rare among rodents. We digitized a total of 1125 crania, representing 309 species of muroid rodents and outgroups (Fig. 1), using a Microscribe MX5 3D stylus digitizer (see the electronic supplementary material, Table S3). Eight sampled species were split into separate Operational Taxonomic Units (OTUs; e.g. *Aegialomys xantheolus* Ecuador vs. *Aegialomys xantheolus* Peru) because the nominate species were not monophyletic on the phylogeny, and consequently the morphological data collected from individuals attributed to each species were applied to both OTUs in each pair (i.e. data collected for all individuals identified as *Aegialomys xantheolus* were applied to both *Aegialomys xantheolus* Ecuador and *Aegialomys xantheolus* Peru). This data duplication assumed that the genetic lineages were nearly indistinguishable for the cranial traits we measured; that is, they represented cryptic species more similar morphologically to each other than to any of the other measured species.

Digitized specimens come from the United States National Museum of Natural History (USNM), the Field Museum of Natural History (FMNH), the Museum of Vertebrate Zoology, Berkeley (MVZ), the University of Florida Museum of Natural History (UF), the American Museum of Natural History (AMNH), Laboratorio de Citogenetica Mamíferos, Universidad de Chile (LCM), and the Oklahoma Museum of Natural History (OMNH). Only wild caught adult individuals were included as diagnosed by the basioccipital–basisphenoid epiphyseal fusion as in Robertson and Shadle (1954) as well as the complete eruption of both 3rd molars as indicated by evidence of occlusal wear (Steppan 1997).

Three dimensional coordinates of 34 landmarks on the crania were captured using the microscribe digitizer, which is accurate to 0.002 mm. Landmarks were chosen to cover most regions of the skull while prioritizing features that are conserved across muroids (Fig. 2; see the electronic supplementary material, Table S4). For more details, see Alhajeri (2014).

Each landmark was digitized multiple times until a precision of 0.3 mm was achieved while retaining the two coordinates with the smallest Euclidean distance between each other. The crania were digitized in two orientations and the data points were merged using generalized Procrustes analysis (GPA; Rohlf and Slice 1990) on common points digitized in both orientations (BR, PT, and APT, see the electronic supplementary material, Table S4) using Morpheus et al. (Slice 2009) followed by the restoration of scale. A complete description of the data merging process appears in the electronic supplementary material, Table S5. Analyses on the first 100 crania showed no significant asymmetry (data not shown), and therefore crania were subsequently digitized and analyzed on the left side only. Cardini (2016) showed that at the macroevolutionary scale (as in this study), results from analyzing one side of a bilaterally symmetric structure (e.g. skull) was highly congruent to results of analyzing both sides; congruence was less at the intraspecific level.

A detailed description of the taxonomic sampling strategy, microscribe data collection and processing procedures, and an overview and reasoning behind the choice of the three-dimensional landmarks were described in Alhajeri (2014).

Geometric Morphometric Methods

The crania were vetted to include only those that were in the best condition, however, 368 out of the 1125 digitized specimens had at least one missing landmark (see the electronic supplementary material, Table S6) because of damage or due to not being identifiable in the species. These missing landmark coordinates were estimated in the GEOMORPH library (Adams and Otárola-Castillo 2013) in R using thin-plate spline interpolation on landmarks common to both complete specimens and those with missing data (see the electronic supplementary material, Table S5).

To obtain GM shape and size variables, we conducted GPA on the complete dataset, a method that involves rescaling, translation, and rotation of coordinate configurations in order minimize differences from an iteratively estimated consensus configuration (which in turn is updated after each transformation) (Zelditch et al. 2004). The output of this superimposition are configurations of the same size, or Procrustes coordinates (PrC), that describe shape differences within the sample, as well as centroid-size (CS), which is sequestered in a separate variable. The first GPA outputted PrC and CS for all specimens. CS from this GPA were averaged, and log transformed for each species and used as an estimate of GM size, while PrC was subjected to another GPA for each group of conspecifics to align specimens prior to estimating species average shape. Average shape was estimated using the method described in Claude (2008), which calculates the average coordinate positions of aligned

Table 1 Clade information for the four chronological sampling intervals

Age (mya)	# Clades	Mean	Range	SD
5	36	31.2	6–127	28.7
7.5	25	51.7	6–151	46.9
10	14	106.2	6–576	168.4
12.5	7	218	17–681	287.8

Clade # is based on clades where at least three species appear in the morphological dataset, not total species number. The mean, range, and standard deviation of species numbers per clade are indicated

specimens as implemented in the GEOMORPH library in R. The resulting species consensus shapes were subjected to another GPA to re-align. The output of this GPA is a set of PrC that describe interspecific shape variation within the sample.

We applied a principal component analysis (PCA) on PrC (i.e. relative warp analysis) to reduce the number of shape variables (34 landmarks in 3D = 102 PrC) and to simplify interpretation. The resulting relative warps (RW) provide a summary of the greatest aspects of shape variation that are listed in decreasing importance and are also orthogonal (see the electronic supplementary material, Table S7). PCA was conducted in the PCAMETHODS library (Stacklies et al. 2007) in R using singular value decomposition. The distribution of families in morphospace was visualized on RW1–6 which together explain 54.1% of the cranial shape variance (Table 3). The distribution of species in cranial shape morphospace based on all shape information (102 PrC) was visualized using a dendrograms based on hierarchical cluster analysis on the squared Euclidean distance matrix using Ward's method (Sneath and Sokal 1973) as implemented in R base package.

Extraction of Linear Distances

In addition to GM, we also quantified morphology by extracting linear distances from coordinate data. This was done by calculating distances between coordinates in raw specimen data that did not undergo any GM process prior to calculating species averages. Consequently, scale was preserved, and measurements are comparable to other studies that use distance-based approaches. Linear distances were based on Marroig and Cheverud (2001), Cheverud (1995), and Steppan (1997) and are summarized in the electronic supplementary material, Table S8, and were log-transformed prior to PCA. Linear distance loadings indicate that PC1 was a size-vector because the loadings were of the same sign (negative) and of similar magnitudes whereas PCs 2–39 are shape vectors because for all of them, the loadings differed among the distance variables in magnitude and sign (see the electronic supplementary material, Table S9). As in the GM

analyses above, the distribution of families in morphospace was visualized using PC1–6 that together explain 90.7% of the morphological variation (Table 4). The distribution of species in cranial morphospace based on PC2–39 was visualized using dendrograms.

Morphological Disparity and Evolution Rate Estimates

Disparity and evolutionary rate within clades was also quantified. Disparity is defined as the variance in morphospace among species (Foote 1993) and total disparity for each clade is calculated as the average squared Euclidean distance among all pairs of species in the morphological datasets (the optimal method for datasets that are in the same units; Harmon et al. 2008) as implemented in the GEIGER library in R. Depending on the distribution of morphological variation within subclades, the evolutionary rate (a measure of change through time) may result in a widely different value than disparity, with high rates indicating over-dispersion of similar morphologies and a low values indicating clustering of similar morphologies (O'Meara et al. 2006); and disparity measures being unaffected.

We compared the fit of the Brownian motion (BM) model of evolution to the Ornstein–Uhlenbeck (OU) model for each trait/clade combination in the MVMORPH library (Clavel 2014) in R using the Akaike Information Criterion (AIC; Akaike 1974). For all combinations, the BM model fit the data best, and/or the rates of evolution estimated by the two models were similar (data not shown). Therefore, the BM model was used to calculate the maximum-likelihood estimates of morphological evolution rates (σ^2) for all trait/clade combinations. A multivariate BM model was fit to the two shape datasets (102 PrCs/PC2–39) and a univariate model was fit to the size datasets (log CS/PC1) as implemented in the MVMORPH library in R. For the multivariate model, an estimate of the overall rate of evolution of the variables was calculated as the sum of the individual rates of each variable, or the trace of the rate matrix (as in Adams et al. 2009).

Log richness/diversification rates (Table 2) were regressed onto disparity/evolution rates (Table 5) calculated using: (1) GM shape based on all PrC data; (2) GM size based on log-transformed CS; (3) LM shape based on PC2–39; and (4) LM size based on PC1.

Correlation Between Diversity and Disparity/Evolutionary Rate

The association between diversity and disparity/evolutionary rate was tested using PGLS (Martins and Hansen 1997) to account for the non-independence of clades because of their phylogenetic relatedness, using subclade trees extracted from the chronogram described above as

Table 2 Summary of diversity and diversification rate estimates

	Species #			Age	Log richness	Diversification rate
	Sampled	Total	Proportion			
12.5 mya						
1. Dipodidae clade	3	38	0.08	10.27	1.57978	0.26086
2. Spalacidae clade	3	17	0.18	6.82	1.23045	0.27891
3. Nesomyinae	10	23	0.43	10.87	1.36173	0.20173
4. Nesomyidae clade I	12	38	0.32	11.68	1.57978	0.22947
5. Deomyinae + Gerbillinae	29	145	0.20	11.89	2.16137	0.33669
6. Murinae	102	584	0.17	10.61	2.76641	0.50787
7. Cricetidae	151	681	0.22	11.50	2.83315	0.48189
10 mya						
1. Spalacidae clade	3	17	0.18	6.82	1.23045	0.27891
2. Nesomyinae clade I	5	9	0.56	8.63	0.95424	0.15164
3. Nesomyinae clade II	5	14	0.36	7.90	1.14613	0.21750
4. Nesomyidae clade II	3	6	0.50	9.02	0.77815	0.10465
5. Dendromurinae + Cricetomyinae	9	32	0.28	9.23	1.50515	0.27209
6. Deomyinae	9	42	0.21	8.88	1.62325	0.31265
7. Gerbillinae	20	103	0.19	8.57	2.01284	0.42716
8. Murinae clade I	3	8	0.38	6.90	0.90309	0.17392
9. Murinae clade II	99	576	0.17	8.73	2.76042	0.61618
10. Cricetinae	6	18	0.33	7.97	1.25527	0.24568
11. Arvicolinae	22	151	0.15	5.75	2.17898	0.70353
12. Neotominae	31	124	0.25	8.70	2.09342	0.44209
13. Tylomyinae	4	10	0.40	8.44	1.00000	0.16641
14. Sigmodontinae	88	377	0.23	8.34	2.57634	0.59375
7.5 mya						
1. Spalacidae clade	3	17	0.18	6.82	1.23045	0.27891
2. Nesomyinae clade III	3	6	0.50	6.68	0.77815	0.14133
3. Nesomyinae clade IV	4	12	0.33	6.36	1.07918	0.24759
4. Dendromurinae clade	4	13	0.31	6.14	1.11394	0.26880
5. Deomyinae clade	4	22	0.18	6.63	1.34242	0.32441
6. <i>Acomys</i>	4	19	0.21	6.23	1.27875	0.32256
7. Gerbillinae clade I	5	16	0.31	6.57	1.20412	0.28094
8. Gerbillinae clade II	13	80	0.16	6.16	1.90309	0.55404
9. Murinae clade I	3	8	0.38	6.90	0.90309	0.17392
10. Murinae clade III	26	149	0.17	5.87	2.17319	0.68659
11. Murinae clade IV	25	119	0.21	5.99	2.07555	0.63494
12. Murinae clade V	19	86	0.22	6.25	1.93450	0.55738
13. <i>Apodemus</i>	5	20	0.25	5.67	1.30103	0.36322
14. <i>Mus</i>	7	38	0.18	5.18	1.57978	0.51763
15. Murinae clade VI	11	44	0.25	4.73	1.64345	0.59744
16. Cricetinae clade	4	9	0.44	4.17	0.95424	0.31391
17. Arvicolinae	22	151	0.15	5.75	2.17898	0.70353
18. Neotominae clade I	6	24	0.25	5.56	1.38021	0.40174
19. Neotominae clade II	22	93	0.24	6.15	1.96848	0.57952
20. Tylomyinae clade	3	8	0.38	4.04	0.90309	0.29708
21. Sigmodontinae clade I	5	24	0.21	7.18	1.38021	0.31110
22. Sigmodontinae clade II	7	55	0.13	6.64	1.74036	0.45817
23. Sigmodontinae clade III	27	129	0.21	6.37	2.11059	0.61028
24. Sigmodontinae clade IV	17	81	0.21	5.76	1.90849	0.59406

Table 2 (continued)

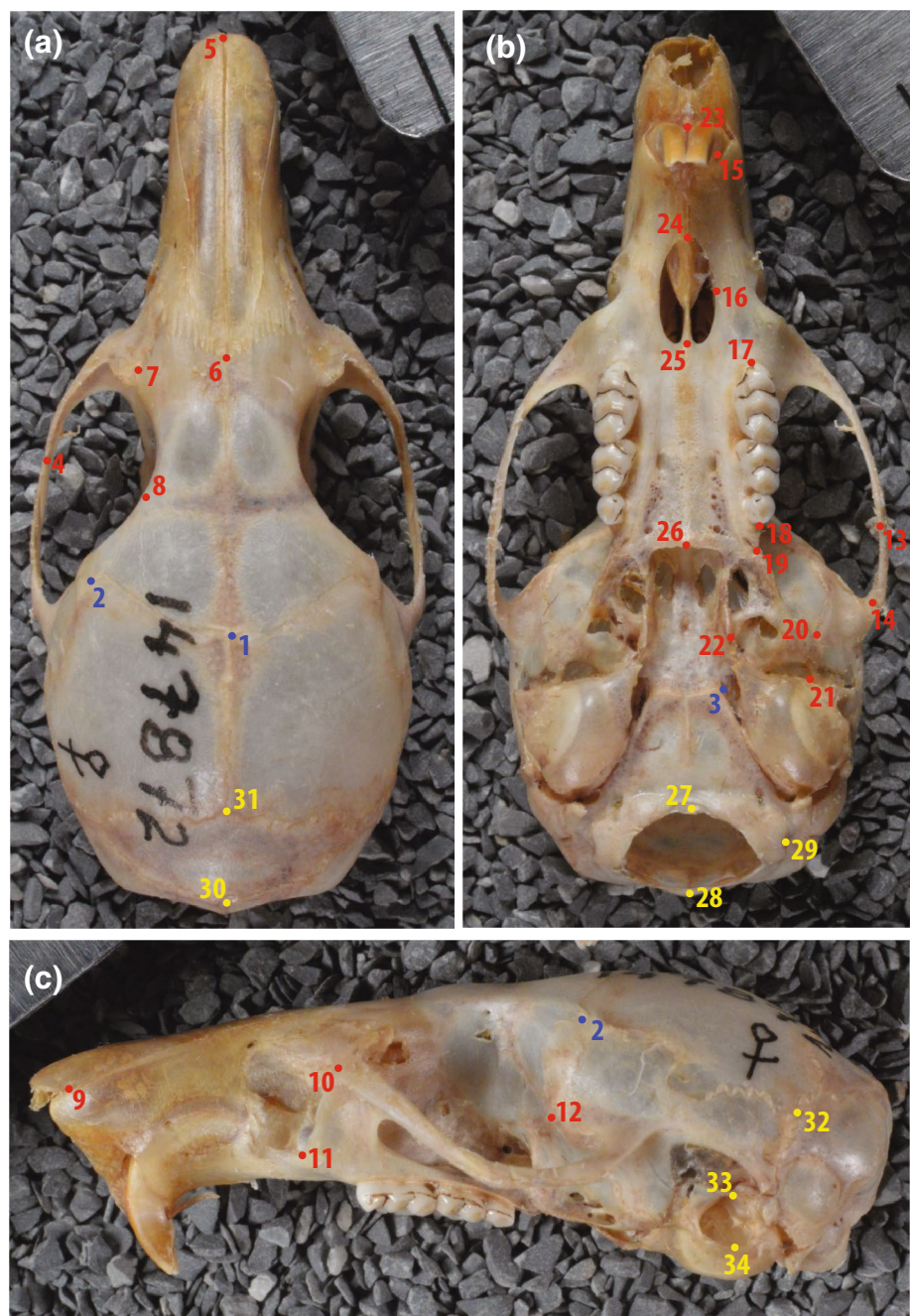
	Species #			Age	Log richness	Diversification rate
	Sampled	Total	Proportion			
25. Sigmodontinae clade V 5 mya	29	70	0.41	6.86	1.84510	0.47824
1. Nesomyinae clade V	3	11	0.27	4.41	1.04139	0.33884
2. <i>Dendromys</i>	3	12	0.25	1.53	1.07918	1.02812
3. <i>Lophuromys</i>	3	21	0.14	2.73	1.32222	0.76961
4. <i>Acomys</i> subclade	3	17	0.18	3.66	1.23045	0.52015
5. Gerbillinae clade III	3	14	0.21	4.31	1.14613	0.39867
6. Gerbillinae clade IV	6	20	0.30	3.92	1.30103	0.52505
7. Gerbillinae clade V	6	52	0.12	4.75	1.71600	0.62937
8. Murinae clade VII	3	21	0.14	4.06	1.32222	0.51823
9. Murinae clade VIII	26	127	0.20	4.79	2.10380	0.80769
10. Murinae clade IX	5	17	0.29	4.49	1.23045	0.42342
11. Murinae clade X	3	7	0.43	4.49	0.84510	0.24044
12. Murinae clade XI	13	94	0.14	4.55	1.97313	0.78425
13. Murinae clade XII	3	21	0.14	3.00	1.32222	0.70089
14. Murinae clade XIII	4	21	0.19	4.71	1.32222	0.44706
15. Murinae clade XIV	6	22	0.27	4.20	1.34242	0.51200
16. <i>Apodemus</i> subclade	3	18	0.17	4.55	1.25527	0.42968
17. <i>Mus</i> subclade	5	36	0.14	3.64	1.55630	0.72267
18. Murinae clade VI	11	44	0.25	4.73	1.64345	0.59744
19. Cricetinae clade	4	9	0.44	4.17	0.95424	0.31391
20. Arvicolinae clade I	4	17	0.24	4.71	1.23045	0.40392
21. Arvicolinae clade II	15	108	0.14	4.55	2.03342	0.81494
22. <i>Neotoma</i>	4	22	0.18	3.52	1.34242	0.61006
23. <i>Reithrodontomys</i>	4	20	0.20	4.40	1.30103	0.46814
24. Neotominae clade III	16	67	0.24	4.15	1.82607	0.78024
25. Tylomyinae clade	3	8	0.38	4.04	0.90309	0.29708
26. <i>Sigmodon</i>	3	14	0.21	3.94	1.14613	0.43626
27. <i>Thomasomys</i>	4	36	0.11	3.71	1.55630	0.70721
28. Sigmodontinae clade VI	6	30	0.20	4.42	1.47712	0.55428
29. Sigmodontinae clade VII	5	28	0.18	4.67	1.44716	0.51016
30. Sigmodontinae clade VIII	13	67	0.19	4.68	1.82607	0.69106
31. Sigmodontinae clade IX	5	13	0.38	4.95	1.11394	0.33341
32. Sigmodontinae clade X	10	52	0.19	3.85	1.71600	0.77621
33. Sigmodontinae clade XI	3	6	0.50	4.44	0.77815	0.21249
34. Sigmodontinae clade XII	5	14	0.36	3.49	1.14613	0.49205
35. <i>Calomys</i>	3	12	0.25	3.81	1.07918	0.41364
36. Sigmodontinae clade XIII	12	25	0.48	4.88	1.39794	0.46612

Descriptions of clades in the first columns are in supporting electronic supplementary material, Table S2. Clades are listed in the same order as they appear from the bottom to the top of Fig. 1, with the numbers preceding the clades indicating their identification number in the regression plots below (only outliers are highlighted in the plots)

implemented in the CAPER library (Orme et al. 2013) in R. This tested the null hypothesis that all measures of diversity are uncorrelated with disparity/evolutionary rate and the alternate hypothesis, based on theory, of a positive correlation. We used PGLS to test the association between: (A) log richness vs. disparity calculated using GM and LM

size and shape datasets and at different clade designations; (B) diversification rate vs. evolution rate also calculated using GM and LM size and shape datasets and similarly with different clade designations. This setup also facilitated testing whether the association between diversity and disparity/evolutionary rate was affected by variation in:

Fig. 2 Positions of three dimensional cranial landmarks. Landmarks are shown on the **a** dorsal, **b** ventral, and **c** lateral views of the Mount Apo Forest Mouse (*Apomys hylacoetes*; FMNH 147872) with numbers corresponding to descriptions in supporting electronic supplementary material, Table S4. Landmarks in red are digitized in the anterior orientation, those in yellow are digitized in the posterior orientation, and those in blue are digitized in both orientations and used to merge the data from the two orientations. The jugular process is missing in this specimen and landmark 29 is positioned where it is commonly present. (Color figure online)



(1) morphological data character types (GM vs. LM); (2) size versus shape datasets; (3) time intervals for extracting clades; and (4) estimates of diversity (log richness vs. diversification rates) and disparity versus evolution rate. We also examined the relationship between: clade age versus log richness and disparity; diversification rate versus log richness and disparity; evolution rate versus disparity and log richness; size disparity/evolution rate versus shape disparity/evolution rate (both within and across GM and LM datasets).

Results

Dispersion in Morphospace

There was extensive overlap in cranial size both based on GM (Fig. 3a) and LM (Fig. 3b); both these approaches showed the same relative relationships in average size. Since all the linear distances load negatively onto PC1 (see the electronic supplementary material, Table S9),

Table 3 Proportion of explained variance by RW1–102

	R ²	Cumulative R ²
RW1	.1651	.1651
RW2	.1025	.2676
RW3	.0791	.3467
RW4	.0754	.4221
RW5	.0700	.4921
RW6	.0492	.5413
RW7	.0415	.5828
RW8	.0382	.6210
RW9	.0367	.6578
RW10	.0320	.6898
RW11	.0280	.7178
RW12	.0256	.7434
RW13	.0200	.7633
RW14	.0188	.7821
RW15	.0157	.7978
RW16–102	.2022	1.0000

Both the individual and the cumulative explained variance are indicated

Table 4 Proportion of variance explained by PC1–39

	R ²	Cumulative R ²
PC1	.7329	.7329
PC2	.0558	.7887
PC3	.0403	.8290
PC4	.0340	.8630
PC5	.0243	.8873
PC6	.0200	.9073
PC7	.0134	.9207
PC8	.0116	.9323
PC9	.0094	.9416
PC10	.0076	.9493
PC11	.0074	.9566
PC12	.0061	.9627
PC13	.0048	.9675
PC14	.0043	.9718
PC15	.0040	.9757
PC16–39	.0243	1.0000

See Table 3 for more information

a decrease in the score of PC1 indicates an increase in cranial size. Spalacids have the largest crania, followed jointly by murids + cricetids + dipodids + nesomyids, and lastly the sole calomyscid and platacanthomyid, with the smallest crania (Fig. 3a, b).

There was also extensive overlap in cranial shape based on both GM (Fig. 4a–c) and LM (Fig. 4d–f) approaches. The cricetids and the murids show the greatest morphological

variation in all examined axes, with almost complete overlap in morphology. All other families, including the one sampled calomyscid, are mostly nested within this region of overlap, except for the sole platacanthomyid in RW3 versus RW4 (Fig. 4b) where it falls out of this region. The other three families with more than one sampled representative (nesomyids, dipodids, and spalacids) have considerably less morphological diversity and more distinctive occupation in morphospace. Nesomyids overlapped extensively with all families (including dipodids and spalacids) in all examined axes except RW1 and RW2 where they are clearly separated from dipodids and spalacids (Fig. 4a). Dipodids and spalacids overlapped less extensively with each other (although they did overlap considerably with other families). This is especially evident on RW1 and RW2 (Fig. 4a), RW5 and RW6 (Fig. 4c), PC1 and PC2 (Fig. 4d), and PC4 (Fig. 4e). When total data was visualized using dendrograms, genera cluster together in morphospace in both GM (see the electronic supplementary material, Fig. S1) and LM (see the electronic supplementary material, Fig. S2) more often than not. This pattern indicates that some component of the interspecific cranial shape variation is independent of size.

Diversity and Disparity/Evolutionary Rate Regressions

Clade diversity was not significantly correlated with disparity (Table 6; Fig. 5a–d) and diversification rate was not significantly correlated with morphological evolution rate (Table 6; Fig. 5e–h) for both GM and LM size and shape datasets and across all four investigated time periods (5–12.5 mya). Clade diversity was also not significantly correlated with morphological evolution rate and clade diversification rate was not significantly correlated with disparity (results not shown). Clade age was not significantly correlated with disparity (Table 6; Fig. 6a–d) for both GM and LM size and shape datasets and across all time periods. Clade morphological evolution rate was highly correlated with disparity (Table 6; Fig. 6e–h) for all the GM and LM size and shape datasets and across all time periods except for GM shape disparity versus GM shape evolution rate at 12.5 and 10 mya. Clade age was not significantly correlated with diversity (Table 6; Fig. 6i) across all time periods and diversification rates were significantly correlated diversity (Table 6; Fig. 6j) for all time periods.

Alternative measures of disparity were often, but not always, correlated with each other. At 5 mya, GM shape disparity was highly correlated with GM size disparity ($p < 0.0001$, $R^2 = 0.701$) but LM shape disparity was not correlated with LM size disparity ($p = 0.764$, $R^2 = 0.0027$), possibly because size-dependent shape changes (allometry) can be retained in the GM shape while removed in the LM PCs 2–39. GM shape disparity was correlated

Table 5 Summary of disparity and evolution rate estimates based on four morphological datasets

	Disparity				σ^2			
	PrC	log CS	PC2–39	PC1	PrC	log CS	PC2–39	PC1
12.5 mya								
1. Dipodidae clade	0.02498	0.01333	0.23529	0.10435	0.00082	0.00043	0.00792	0.00356
2. Spalacidae clade	0.01684	0.01983	0.24071	0.73919	0.00099	0.00120	0.01436	0.04775
3. Nesomyinae	0.01255	0.03639	0.11491	1.52889	0.00080	0.00208	0.00843	0.08135
4. Nesomyidae clade I	0.01753	0.04495	0.32377	1.33408	0.00182	0.00212	0.06099	0.14736
5. Deomyinae + Gerbillinae	0.02033	0.01085	0.22352	0.43526	0.00162	0.00047	0.02434	0.04474
6. Murinae	0.01728	0.03523	0.22801	0.80083	0.00159	0.00244	0.02073	0.05433
7. Cricetidae	0.02092	0.01723	0.24364	0.50507	0.00221	0.00115	0.02632	0.03479
10 mya								
1. Spalacidae clade	0.01684	0.01983	0.24071	0.73919	0.00099	0.00120	0.01436	0.04775
2. Nesomyinae clade I	0.01326	0.05761	0.11926	2.20291	0.00084	0.00235	0.00924	0.09313
3. Nesomyinae clade II	0.00911	0.02297	0.09656	1.03058	0.00068	0.00180	0.00690	0.06789
4. Nesomyidae clade II	0.02258	0.04630	0.11954	1.16731	0.00088	0.00183	0.00513	0.05522
5. Dendromurinae + Cricetomyinae	0.01586	0.04866	0.39556	1.48454	0.00207	0.00212	0.07929	0.17504
6. Deomyinae	0.01142	0.00246	0.10704	0.15393	0.00113	0.00013	0.01795	0.07304
7. Gerbillinae	0.01497	0.01159	0.21262	0.49551	0.00177	0.00058	0.02665	0.03083
8. Murinae clade I	0.02645	0.06192	1.18144	1.88616	0.00126	0.00283	0.06350	0.08741
9. Murinae clade II	0.01683	0.03341	0.17340	0.78560	0.00159	0.00237	0.01840	0.05353
10. Cricetinae	0.01073	0.01993	0.28799	0.36782	0.00081	0.00179	0.02204	0.03377
11. Arvicolinae	0.01208	0.02030	0.13949	0.48303	0.00141	0.00157	0.01603	0.03684
12. Neotominae	0.00864	0.02558	0.11792	0.85787	0.00099	0.00113	0.01232	0.04247
13. Tylomyinae	0.00670	0.00883	0.16920	0.19559	0.00034	0.00031	0.00953	0.00676
14. Sigmodontinae	0.02000	0.01334	0.22871	0.37605	0.00298	0.00104	0.03442	0.03251
7.5 mya								
1. Spalacidae clade	0.01684	0.01983	0.24071	0.73919	0.00099	0.00120	0.01436	0.04775
2. Nesomyinae clade III	0.01452	0.04177	0.15361	1.93572	0.00077	0.00201	0.00867	0.08920
3. Nesomyinae clade IV	0.00713	0.01748	0.10170	0.56502	0.00064	0.00176	0.00763	0.05494
4. Dendromurinae clade	0.01253	0.00189	0.08074	0.07606	0.00322	0.00055	0.01396	0.00637
5. Deomyinae clade	0.00826	0.00206	0.08858	0.20501	0.00137	0.00010	0.02587	0.15896
6. <i>Acomys</i>	0.00608	0.00096	0.09216	0.02612	0.00070	0.00006	0.01159	0.00163
7. Gerbillinae clade I	0.01323	0.00838	0.11497	0.16236	0.00128	0.00057	0.01091	0.01186
8. Gerbillinae clade II	0.01498	0.01405	0.25234	0.68245	0.00206	0.00061	0.03520	0.04069
9. Murinae clade I	0.02645	0.06192	1.18144	1.88616	0.00126	0.00283	0.06350	0.08741
10. Murinae clade III	0.01099	0.01637	0.13465	0.34919	0.00154	0.00215	0.02109	0.04666
11. Murinae clade IV	0.02962	0.04834	0.23445	0.94575	0.00292	0.00535	0.02682	0.10173
12. Murinae clade V	0.01131	0.00593	0.14082	0.21977	0.00099	0.00037	0.01306	0.01963
13. <i>Apodemus</i>	0.00514	0.00192	0.05278	0.25736	0.00041	0.00013	0.00408	0.02302
14. <i>Mus</i>	0.00740	0.00523	0.08313	0.10224	0.00088	0.00048	0.00940	0.01039
15. Murinae clade VI	0.00581	0.00530	0.10764	0.15524	0.00077	0.00041	0.01496	0.02693
16. Cricetinae clade	0.00790	0.02137	0.26103	0.40344	0.00079	0.00217	0.02367	0.04315
17. Arvicolinae	0.01208	0.02030	0.13949	0.48303	0.00141	0.00157	0.01603	0.03684
18. Neotominae clade I	0.00740	0.00403	0.10147	0.20903	0.00091	0.00043	0.01466	0.01769
19. Neotominae clade II	0.00692	0.01013	0.09841	0.47840	0.00104	0.00096	0.01215	0.04203
20. Tylomyinae clade	0.00407	0.00123	0.14515	0.01595	0.00028	0.00008	0.00989	0.00109
21. Sigmodontinae clade I	0.03064	0.00635	0.24207	0.25490	0.00235	0.00037	0.01993	0.02569
22. Sigmodontinae clade II	0.00964	0.00408	0.10615	0.06373	0.00094	0.00053	0.00845	0.00678
23. Sigmodontinae clade III	0.01232	0.02066	0.15370	0.63612	0.00148	0.00155	0.02216	0.06091
24. Sigmodontinae clade IV	0.01961	0.01852	0.22999	0.48862	0.00568	0.00136	0.06474	0.03542

Table 5 (continued)

	Disparity				σ^2			
	PrC	log CS	PC2–39	PC1	PrC	log CS	PC2–39	PC1
25. Sigmodontinae clade V	0.02050	0.00615	0.23376	0.10044	0.00339	0.00058	0.03789	0.01080
5 mya								
1. Nesomyinae clade V	0.00745	0.01944	0.10288	0.55576	0.00071	0.00198	0.00798	0.05800
2. <i>Dendromys</i>	0.00908	0.00131	0.06269	0.01160	0.00391	0.00067	0.01627	0.00429
3. <i>Lophuromys</i>	0.00280	0.00005	0.06422	0.28979	0.00146	0.00001	0.03193	0.21156
4. <i>Acomys</i> subclade	0.00688	0.00028	0.11754	0.00967	0.00083	0.00002	0.01457	0.00080
5. Gerbillinae clade III	0.01049	0.00859	0.09660	0.08742	0.00131	0.00060	0.01169	0.00798
6. Gerbillinae clade IV	0.01420	0.00355	0.25430	0.36175	0.00199	0.00042	0.03682	0.05504
7. Gerbillinae clade V	0.01484	0.00419	0.26176	0.06916	0.00220	0.00037	0.03630	0.00853
8. Murinae clade VII	0.01297	0.01034	0.20324	0.09627	0.00106	0.00081	0.01612	0.00757
9. Murinae clade VIII	0.00891	0.01517	0.20324	0.32051	0.00150	0.00224	0.02180	0.04824
10. Murinae clade IX	0.02034	0.01149	0.12420	0.22002	0.00197	0.00126	0.02000	0.02323
11. Murinae clade X	0.09223	0.08910	0.20666	1.83002	0.00634	0.00606	0.00852	0.12302
12. Murinae clade XI	0.01937	0.05052	0.10753	0.85657	0.00228	0.00619	0.03362	0.10790
13. Murinae clade XII	0.00866	0.00036	0.24149	0.06442	0.00104	0.00005	0.01379	0.00702
14. Murinae clade XIII	0.01105	0.00115	0.11659	0.10077	0.00096	0.00011	0.01469	0.00764
15. Murinae clade XIV	0.00587	0.00315	0.16805	0.12627	0.00069	0.00031	0.00994	0.02175
16. <i>Apodemus</i> subclade	0.00637	0.00032	0.05126	0.46464	0.00048	0.00002	0.00381	0.03580
17. <i>Mus</i> subclade	0.00837	0.00453	0.09415	0.08370	0.00104	0.00042	0.01101	0.00926
18. Murinae clade VI	0.00581	0.00530	0.10764	0.15524	0.00077	0.00041	0.01496	0.02693
19. Cricetinae clade	0.00790	0.02137	0.26103	0.40344	0.00079	0.00217	0.02367	0.04315
20. Arvicolinae clade I	0.01103	0.00784	0.12040	0.33311	0.00097	0.00069	0.01081	0.02706
21. Arvicolinae clade II	0.00966	0.00646	0.11650	0.18248	0.00140	0.00073	0.01602	0.01863
22. <i>Neotoma</i>	0.00664	0.00471	0.09803	0.04954	0.00099	0.00047	0.01735	0.00669
23. <i>Reithrodontomys</i>	0.00649	0.00616	0.07328	0.38444	0.00063	0.00066	0.00779	0.04395
24. Neotominae clade III	0.00612	0.00578	0.07342	0.29996	0.00114	0.00068	0.01272	0.02807
25. Tylomyinae clade	0.00407	0.00123	0.14515	0.01595	0.00028	0.00008	0.00989	0.00109
26. <i>Sigmodon</i>	0.00460	0.00207	0.04741	0.16186	0.00058	0.00016	0.00606	0.01229
27. <i>Thomasomys</i>	0.00912	0.00693	0.05020	0.04984	0.00104	0.00082	0.00546	0.00564
28. Sigmodontinae clade VI	0.00841	0.00688	0.15612	0.25246	0.00111	0.00109	0.02214	0.03809
29. Sigmodontinae clade VII	0.01446	0.00314	0.15661	0.18283	0.00158	0.00076	0.02253	0.01742
30. Sigmodontinae clade VIII	0.00876	0.00873	0.13990	0.32430	0.00147	0.00116	0.02105	0.04016
31. Sigmodontinae clade IX	0.03614	0.02743	0.29080	0.53888	0.01330	0.00168	0.12648	0.07051
32. Sigmodontinae clade X	0.00865	0.00191	0.17683	0.03385	0.00244	0.00063	0.04081	0.00744
33. Sigmodontinae clade XI	0.00983	0.00054	0.09449	0.03858	0.00084	0.00004	0.00781	0.00291
34. Sigmodontinae clade XII	0.03105	0.00539	0.55538	0.05809	0.00452	0.00092	0.08255	0.00724
35. <i>Calomys</i>	0.01848	0.00038	0.21942	0.10256	0.01138	0.00033	0.13118	0.02062
36. Sigmodontinae clade XIII	0.01378	0.00592	0.09334	0.10661	0.00229	0.00054	0.01159	0.01156

PrC = 102 Procrustes coordinates (GM shape); Log CS = centroid size (GM size); PC2–39 = LM shape; PC1 = LM size; σ^2 = evolution rate. See Table 2 for more information

LM shape disparity ($p = 0.019$, $R^2 = 0.151$) and GM size disparity was highly correlated with LM size disparity ($p < 0.0001$, $R^2 = 0.860$). GM shape evolution rate was not correlated with GM size evolution rate ($p = 0.118$, $R^2 = 0.070$) and LM shape evolution rate was not correlated with LM size evolution rate ($p = 0.346$, $R^2 = 0.026$).

GM shape evolution rate was also correlated LM shape evolution rate ($p < 0.0001$, $R^2 = 0.774$) and GM size evolution rate was correlated with LM size evolution rate ($p = 0.0008$, $R^2 = 0.283$). Similar results for GM vs. LM size and shape disparity and evolution rate comparisons were found across all time periods.

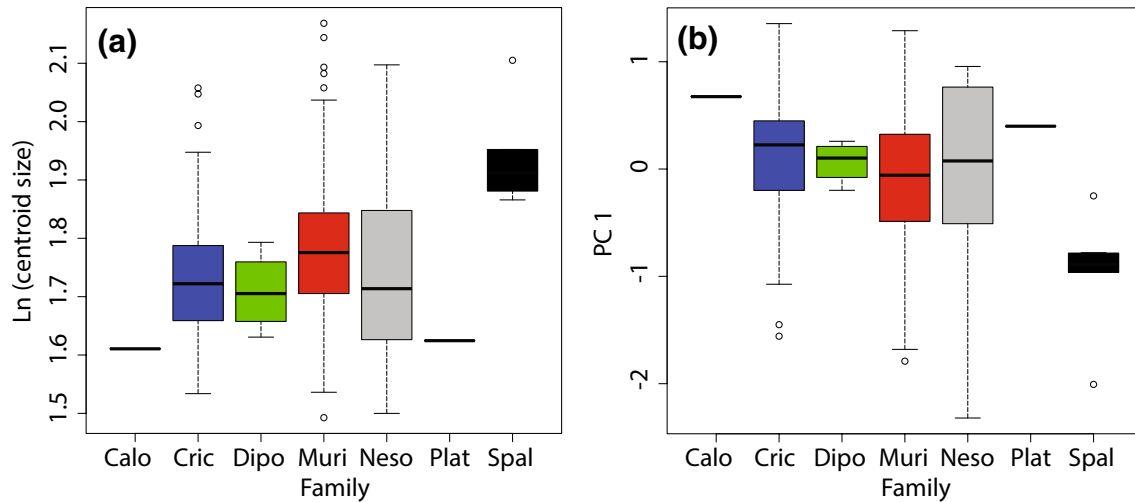


Fig. 3 Dispersion of the seven myodont families in cranial size morphospace based on **a** GM (log CS) and **b** LM (PC1) datasets. Larger values indicate greater size in CS and smaller size in PC1. The first four letters of each family is shown and colors match those in Fig. 4

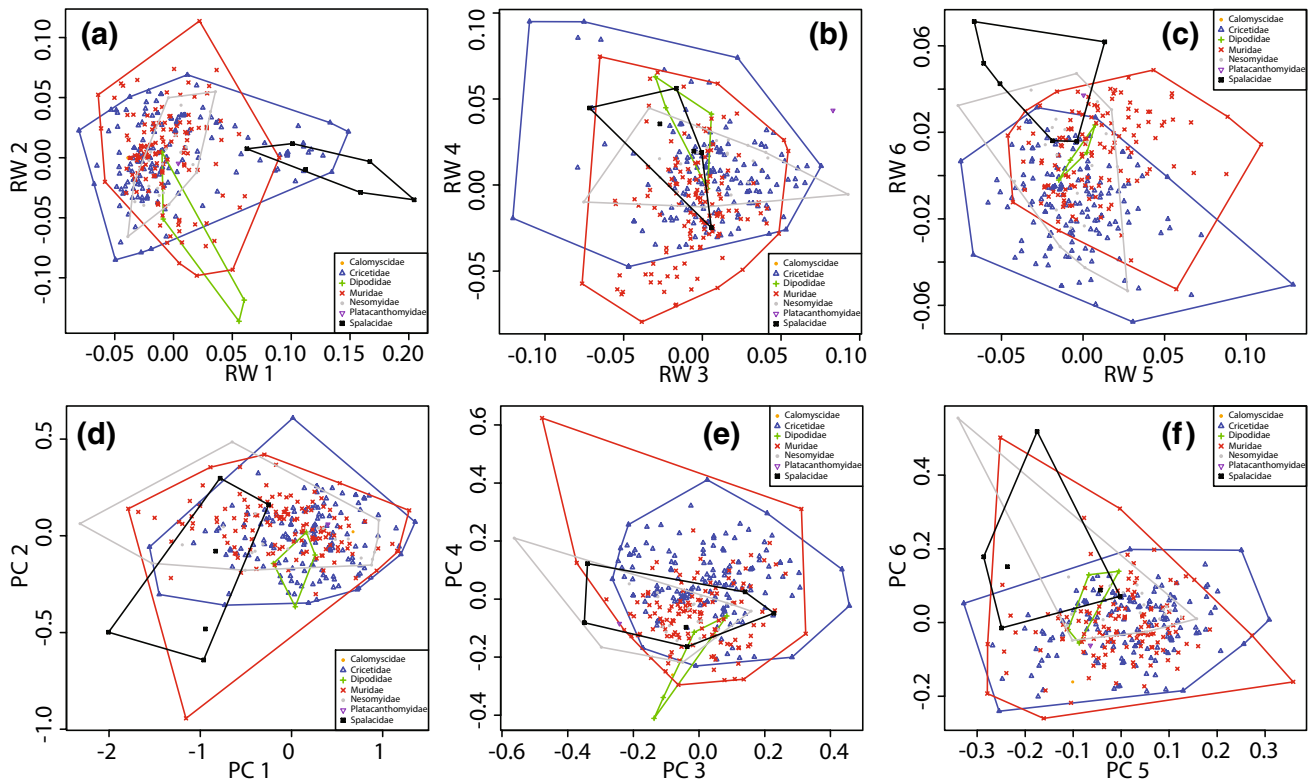


Fig. 4 Dispersion of the seven myodont families in cranial shape morphospace based on **a, b, c** GM (RW1–6) and **d, e, f** LM (PC1–6) datasets. Unlike RW1–6 which are all size independent shape variables, PC1 is a size variable (as in Fig. 3) and PC2–6 are shape vari-

ables. Total variation in shape morphospace is indicated in the dendrograms in supporting electronic supplementary material, Figs. S1 and S2

Table 6 PGLS regression analyses statistical summary

	Time	Estimate	SE	t-Value	R ²	F-Statistic	p-Value
Diversity vs. geometric shape disparity	12.5 mya	0.003	0.002	1.305	.254	1.703	.2487
Diversity vs. geometric shape disparity	10 mya	−0.001	0.002	−0.204	.003	0.042	.8418
Diversity vs. geometric shape disparity	7.5 mya	0.002	0.003	0.634	.017	0.402	.5323
Diversity vs. geometric shape disparity	5 mya	−0.013	0.008	−1.683	.077	2.832	.1016
Diversity vs. geometric size disparity	12.5 mya	−0.003	0.009	−0.322	.020	0.103	.7608
Diversity vs. geometric size disparity	10 mya	−0.011	0.008	−1.463	.151	2.141	.1691
Diversity vs. geometric size disparity	7.5 mya	−0.003	0.007	−0.393	.007	0.154	.6982
Diversity vs. geometric size disparity	5 mya	−0.006	0.008	−0.746	.016	0.557	.4607
Diversity vs. linear shape disparity	12.5 mya	0.012	0.041	0.301	.018	0.091	.7755
Diversity vs. linear shape disparity	10 mya	−0.113	0.120	−0.945	.069	0.893	.3632
Diversity vs. linear shape disparity	7.5 mya	−0.114	0.099	−1.153	.055	1.328	.2609
Diversity vs. linear shape disparity	5 mya	−0.035	0.050	−0.698	.014	0.487	.4900
Diversity vs. linear size disparity	12.5 mya	−0.447	0.250	−1.791	.391	3.208	.1333
Diversity vs. linear size disparity	10 mya	−0.422	0.251	−1.683	.191	2.832	.1182
Diversity vs. linear size disparity	7.5 mya	−0.261	0.230	−1.137	.053	1.292	.2674
Diversity vs. linear size disparity	5 mya	−0.128	0.168	−0.763	.017	0.583	.4506
Diversification rate vs. geometric shape rate	12.5 mya	0.003	0.002	1.860	.409	3.460	.1219
<i>Diversification rate vs. geometric shape rate</i>	<i>10 mya</i>	<i>0.002</i>	<i>0.001</i>	<i>2.630</i>	<i>.366</i>	<i>6.917</i>	<i>.0220</i>
Diversification rate vs. geometric shape rate	7.5 mya	0.002	0.001	1.456	.084	2.119	.1590
Diversification rate vs. geometric shape rate	5 mya	−0.002	0.003	−0.981	.028	0.963	.3334
Diversification rate vs. geometric size rate	12.5 mya	0.001	0.003	0.222	.010	0.049	.8331
diversification rate vs. geometric size rate	10 mya	−0.001	0.001	−0.473	.018	0.224	.6448
Diversification rate vs. geometric size rate	7.5 mya	0.001	0.001	0.764	.025	0.584	.4526
Diversification rate vs. geometric size rate	5 mya	0.000	0.001	0.098	.000	0.010	.9227
Diversification rate vs. linear shape rate	12.5 mya	−0.004	0.067	−0.060	.001	0.004	.9547
Diversification rate vs. linear shape rate	10 mya	−0.001	0.033	−0.020	.000	0.000	.9845
Diversification rate vs. linear shape rate	7.5 mya	0.010	0.019	0.539	.012	0.290	.5952
Diversification rate vs. linear shape rate	5 mya	−0.012	0.026	−0.466	.006	0.217	.6444
Diversification rate vs. linear size rate	12.5 mya	−0.171	0.137	−1.247	.237	1.555	.2677
Diversification rate vs. linear size rate	10 mya	−0.059	0.059	−0.997	.076	0.994	.3385
Diversification rate vs. linear size rate	7.5 mya	−0.021	0.046	−0.445	.009	0.198	.6606
Diversification rate vs. linear size rate	5 mya	0.010	0.038	0.266	.002	0.070	.7922
Clade age vs. diversity	12.5 mya	0.185	0.149	1.244	.236	1.547	.2688
Clade age vs. diversity	10 mya	0.012	0.188	0.062	.000	0.004	.9515
Clade age vs. diversity	7.5 mya	0.043	0.114	0.378	.006	0.143	.7089
Clade age vs. diversity	5 mya	0.110	0.080	1.386	.053	1.921	.1748
Clade age vs. geometric shape disparity	12.5 mya	0.001	0.001	0.624	.072	0.390	.5599
Clade age vs. geometric shape disparity	10 mya	−0.001	0.002	−0.359	.011	0.129	.7257
Clade age vs. geometric shape disparity	7.5 mya	0.005	0.002	3.089	.293	9.544	.0052
Clade age vs. geometric shape disparity	5 mya	0.004	0.004	1.015	.029	1.029	.3175
Clade age vs. geometric size disparity	12.5 mya	0.001	0.003	0.380	.028	0.144	.7199
Clade age vs. geometric size disparity	10 mya	0.001	0.005	0.144	.002	0.021	.8883
Clade age vs. geometric size disparity	7.5 mya	0.004	0.004	1.060	.047	1.124	.3000
Clade age vs. geometric size disparity	5 mya	0.006	0.004	1.578	.068	2.490	.1239
Clade age vs. linear shape disparity	12.5 mya	0.002	0.016	0.112	.003	0.013	.9151
Clade age vs. linear shape disparity	10 mya	−0.089	0.077	−1.154	.100	1.331	.2712
Clade age vs. linear shape disparity	7.5 mya	0.064	0.054	1.174	.056	1.377	.2526
Clade age vs. linear shape disparity	5 mya	0.004	0.024	0.154	.001	0.024	.8787
Clade age vs. linear size disparity	12.5 mya	0.027	0.129	0.208	.009	0.043	.8436
Clade age vs. linear size disparity	10 mya	0.033	0.182	0.181	.003	0.033	.8591

Table 6 (continued)

	Time	Estimate	SE	t-Value	R ²	F-Statistic	p-Value
Clade age vs. linear size disparity	7.5 mya	0.202	0.123	1.643	.105	2.698	.1141
Clade age vs. linear size disparity	5 mya	0.140	0.078	1.780	.085	3.168	.0840
<i>Diversity vs. diversification rate</i>	<i>12.5 mya</i>	<i>4.856</i>	<i>0.601</i>	<i>8.083</i>	<i>.929</i>	<i>65.340</i>	<i>.0005</i>
<i>Diversity vs. diversification rate</i>	<i>10 mya</i>	<i>3.208</i>	<i>0.322</i>	<i>9.971</i>	<i>.892</i>	<i>99.420</i>	<i><.0001</i>
<i>Diversity vs. diversification rate</i>	<i>7.5 mya</i>	<i>2.546</i>	<i>0.168</i>	<i>15.180</i>	<i>.909</i>	<i>230.400</i>	<i><.0001</i>
<i>Diversity vs. diversification rate</i>	<i>5 mya</i>	<i>1.488</i>	<i>0.172</i>	<i>8.670</i>	<i>.689</i>	<i>75.170</i>	<i><.0001</i>
Geometric shape disparity vs. geometric shape rate	12.5 mya	4.321	2.174	1.988	.441	3.950	.1036
Geometric shape disparity vs. geometric shape rate	10 mya	3.743	2.143	1.747	.203	3.051	.1062
<i>Geometric shape disparity vs. geometric shape rate</i>	<i>7.5 mya</i>	<i>3.652</i>	<i>1.046</i>	<i>3.491</i>	<i>.346</i>	<i>12.180</i>	<i>.0020</i>
<i>Geometric shape disparity vs. geometric shape rate</i>	<i>5 mya</i>	<i>3.098</i>	<i>0.772</i>	<i>4.016</i>	<i>.322</i>	<i>16.130</i>	<i>.0003</i>
<i>Geometric size disparity vs. geometric size rate</i>	<i>12.5 mya</i>	<i>15.157</i>	<i>2.682</i>	<i>5.651</i>	<i>.865</i>	<i>31.940</i>	<i>.0024</i>
<i>Geometric size disparity vs. geometric size rate</i>	<i>10 mya</i>	<i>20.286</i>	<i>3.203</i>	<i>6.333</i>	<i>.770</i>	<i>40.110</i>	<i><.0001</i>
<i>Geometric size disparity vs. geometric size rate</i>	<i>7.5 mya</i>	<i>11.354</i>	<i>1.433</i>	<i>7.924</i>	<i>.732</i>	<i>62.800</i>	<i><.0001</i>
<i>Geometric size disparity vs. geometric size rate</i>	<i>5 mya</i>	<i>11.259</i>	<i>0.702</i>	<i>16.042</i>	<i>.883</i>	<i>257.300</i>	<i><.0001</i>
<i>Linear shape disparity vs. linear shape rate</i>	<i>12.5 mya</i>	<i>2.954</i>	<i>0.884</i>	<i>3.343</i>	<i>.691</i>	<i>11.170</i>	<i>.0205</i>
<i>Linear shape disparity vs. linear shape rate</i>	<i>10 mya</i>	<i>9.100</i>	<i>2.559</i>	<i>3.556</i>	<i>.513</i>	<i>12.640</i>	<i>.0040</i>
<i>Linear shape disparity vs. linear shape rate</i>	<i>7.5 mya</i>	<i>9.863</i>	<i>2.025</i>	<i>4.870</i>	<i>.508</i>	<i>23.720</i>	<i>.0001</i>
<i>Linear shape disparity vs. linear shape rate</i>	<i>5 mya</i>	<i>2.000</i>	<i>0.467</i>	<i>4.281</i>	<i>.350</i>	<i>18.330</i>	<i>.0001</i>
<i>Linear size disparity vs. linear size rate</i>	<i>12.5 mya</i>	<i>9.343</i>	<i>2.690</i>	<i>3.474</i>	<i>.707</i>	<i>12.070</i>	<i>.0178</i>
<i>Linear size disparity vs. linear size rate</i>	<i>10 mya</i>	<i>10.145</i>	<i>3.333</i>	<i>3.044</i>	<i>.436</i>	<i>9.265</i>	<i>.0102</i>
<i>Linear size disparity vs. linear size rate</i>	<i>7.5 mya</i>	<i>7.836</i>	<i>2.310</i>	<i>3.393</i>	<i>.334</i>	<i>11.510</i>	<i>.0025</i>
<i>Linear size disparity vs. linear size rate</i>	<i>5 mya</i>	<i>5.040</i>	<i>1.037</i>	<i>4.863</i>	<i>.410</i>	<i>23.640</i>	<i><.0001</i>

Time = clade designations at four time periods. Significant results are italicized. Scatterplots for 5 mya are shown in Figs. 5 and 6

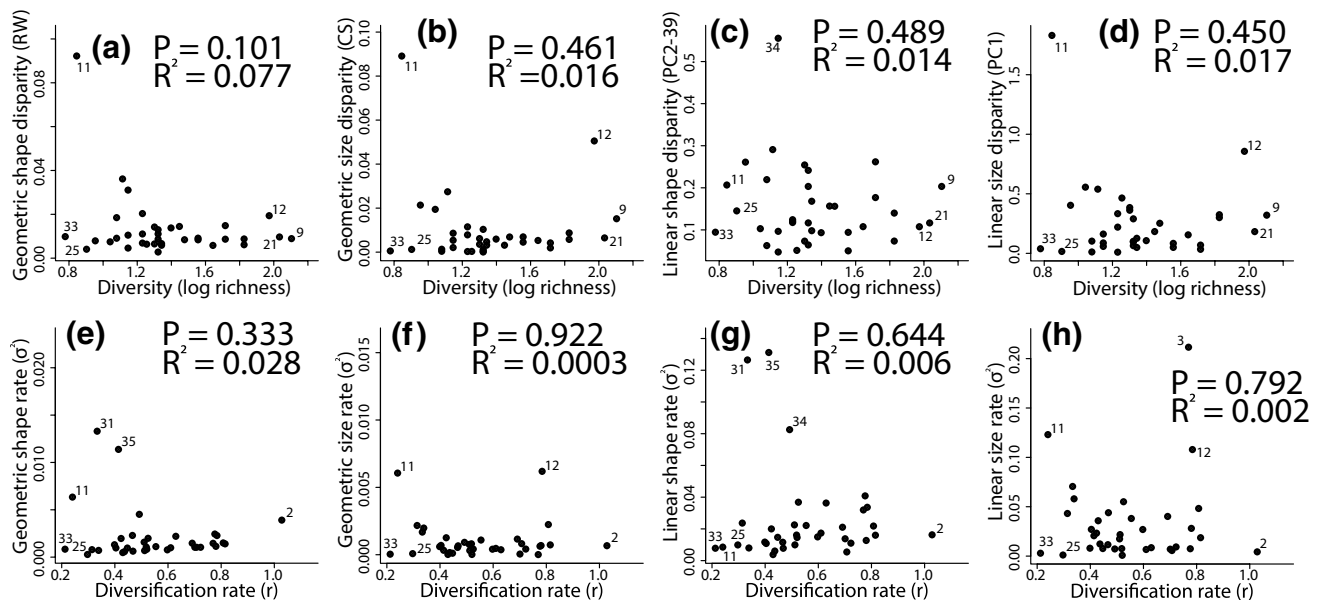


Fig. 5 Linear relationships between **a, b, c, d** diversity versus disparity and **e, f, g, h** diversification rate versus morphological evolution rate of the clades at 5 mya. Several outlier clades are numbers fol-

lowing Tables 2 and 5 and are considered in the discussion. R² and p-values of the PGLS analyses are indicated as in Table 6

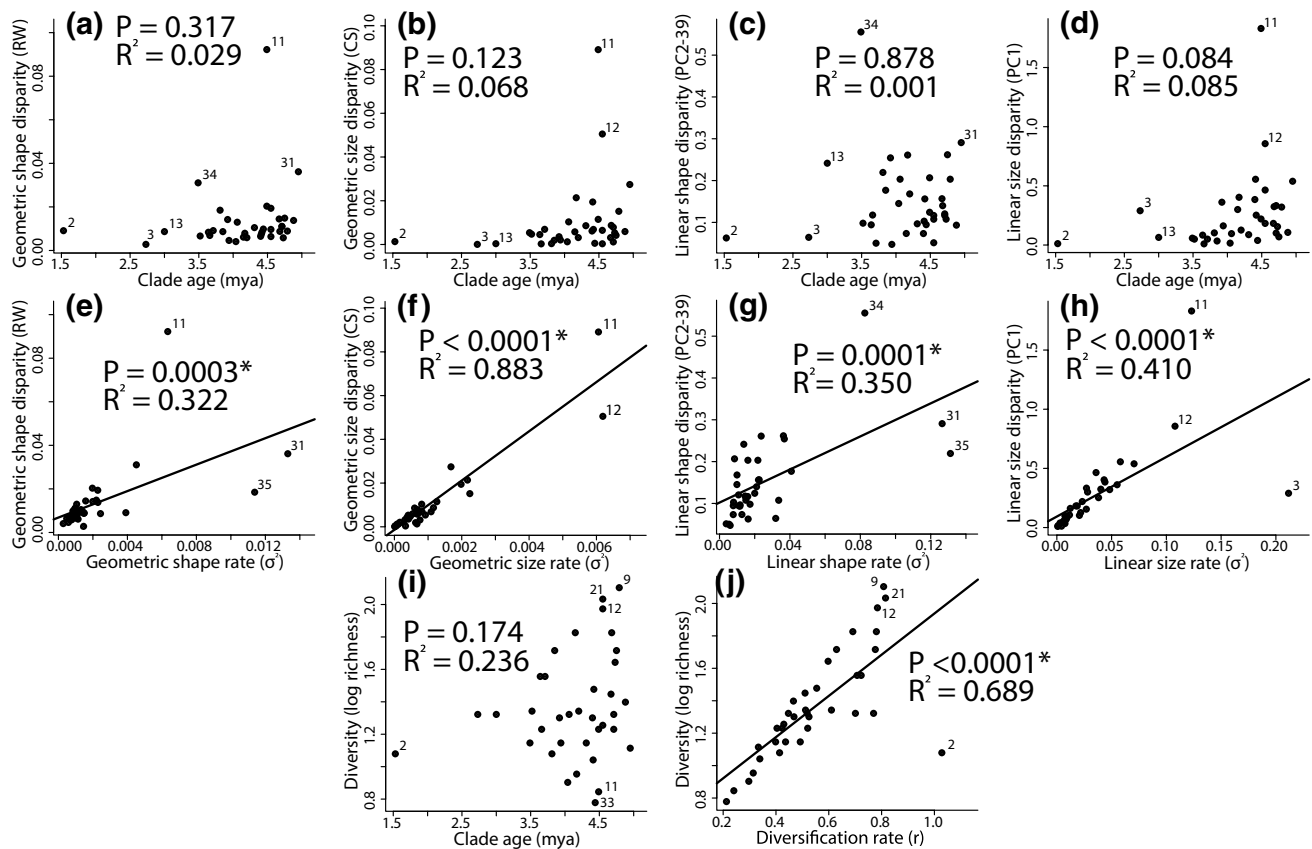


Fig. 6 Linear relationships between **a, b, c, d** clade age versus disparity, **e, f, g, h** morphological evolution rate versus disparity, **(i)** clade age versus diversity and **(j)** diversification rate versus diversity of the clades at 5 mya. See Fig. 5 legend for more information

Discussion

Association Between Diversity and Disparity/Evolutionary Rate in Theory and Empirical Studies

Gould and Eldredge's (1977) punctuated equilibrium model of evolution posits that most phenotypic evolution occurs during speciation events, which are interspersed between longer periods of stasis. If most of the phenotypic change occurs at cladogenesis, then empirically, this model would predict an association between diversity and disparity/evolutionary rate, where lineages that undergo the most speciation events similarly undergo the most phenotypic evolution and vice versa.

Similarly, Schluter's (2000) theory of ecological adaptive radiation also predicts a correlation between diversity and disparity/evolutionary rate in lineages that take advantage of ecological opportunities such as biogeographic transition; which are expected to undergo an early increase in both phylogenetic and phenotypic diversification as they fill available niche space, followed by a density dependent decline in both aforementioned variables as niche space becomes saturated (Simpson 1944; Freckleton and Harvey 2006). The

correlation between these two variables is also supported by simulation studies, where both are positively correlated with clade age, and where older clades have both increased phylogenetic and phenotypic diversity, regardless of diversification and evolution rates (Purvis 2004; Ricklefs 2006).

Empirical support for the association between diversity and disparity/evolutionary rate has been found both with and without phylogenetic framework (e.g. diversity/morphological disparity in passerine birds, Ricklefs 2004; diversity/morphological evolution rate in plethodontid salamanders, Rabosky and Adams 2012; diversification rate/morphological evolution rate in ray-finned fishes; Rabosky et al. 2013). However, other studies indicate that these two variables are uncorrelated (diversification rate/morphological evolution rate in plethodontid salamanders, Adams et al. 2009; diversification rate/morphological disparity in neocete cetaceans; Slater et al. 2010; diversification rate/morphological disparity in *Rattus*; Rowe et al. 2011).

The discrepancy between empirical results suggests that different taxa show different degrees of association between diversity and disparity/evolutionary rate and that other factors such as high extinction rates (e.g. Slater et al. 2010) could impact this pattern of association. This suggests that

the association between these two variables should not always be assumed when testing predictions of theories that assume an association such as the ecological opportunity model of adaptive radiation.

Diversity and Disparity/Evolutionary Rate in Muroid Rodents

The results of this study indicate that diversity and disparity/evolutionary rate are not significantly correlated in muroids. These two variables were not correlated despite (1) the different morphological data character methods (GM vs. LM) employed; (2) the use of both shape and size datasets; (3) extracting clades from different time periods (5, 7.5, 10, and 12.5 mya); and (4) the use of various indices of diversity (log richness and diversification rates) and disparity/evolutionary rate. Results from clades extracted from different time periods were largely consistent; the range of variation in diversity and diversification rates was much greater than that of disparity and morphological evolution rates, with most clades exhibiting relatively low values for the latter (Table 6; Figs. 5, 6). This suggests that in muroids, diversification is accompanied by little morphological divergence; this is supported by the fact that there are many more clades with both low diversity and disparity/evolutionary rate values than there are clades with high values in these two variables.

The three most diverse sampled clades were: Arvicolinae clade II (a geographically widespread vole radiation spanning *Eothenomys* to *Microtus*; see the electronic supplementary material, Table S2), Murinae clade VIII (a Southeast Asian radiation of mostly typical rat generalists spanning *Margaretamys* to *Rattus*), and Murinae clade XI (a highly ecologically diverse Sahulian radiation with highly derived desert, aquatic, and arboreal genera spanning *Leptomys* to *Melomys*). Despite this diversity, Arvicolinae clade II and Murinae clade VIII were no more disparate than most of the other sampled clades in all four indices; however, Murinae clade XI was the second most disparate in both GM and LM size (Table 6; Fig. 5a–d). Similarly, the three least diverse clades were also highly variable in disparities; while Sigmodontinae clade XI (South American group consisting of three genera: chinchilla mice *Chinchillula*, swamp rats *Neotomys*, and climbing mice *Irenomys*) and Tylomyinae clade (South American group consisting of two genera of climbing rats) were among the least disparate in all four indices, Murinae clade X (Sahulian group consisting of two genera of white-eared giant rats *Hyomys* and tree mice *Pogonomys*) is the most disparate in three out of the four indices (GM size, LM size, and GM shape) (Table 6; Fig. 5a–d). The most disparate clade in LM shape is Sigmodontinae clade XII (South American group consisting of four genera of grass mice, long-clawed mole mice, long-clawed Akodonts, and

large long-clawed Akodonts), a clade with moderate to low diversity (Table 6; Fig. 5c).

Similar patterns were observed for the association between the diversification and morphological evolution rates (Table 6; Fig. 5e–h), despite the variation in the identity of the outlier clades. The three least diverse clades (Sigmodontinae clade XI, Tylomyinae clade, and Murinae clade X) also had the lowest diversification rates, however, their morphological evolution rates were not as highly variable as their disparity scores (i.e. Murinae clade X, while having the highest disparity score in most disparity indices, does not have the highest evolution rate, however, it has relatively high values for GM size, LM size, and GM shape) (Table 6; Fig. 5e–h). However, the clade with the highest diversification rate was *Dendromus* (African climbing mice), which was considerably higher than the clades with the highest diversities (Arvicolinae clade II, Murinae clade VIII, and Murinae clade XI), a result most likely attributed to the relatively short branches that separate *Dendromus* members and its recent origin, given that it did not show exceptional diversity and has very low morphological evolution rate (Table 6; Fig. 5e–h). Similarly, the most disparate clades were not necessarily the clades with the greatest morphological evolution rates. While Sigmodontinae clade XII and Murinae clade XI had both high disparity and morphological evolution rate, Sigmodontinae clade IX (South American group consisting of four genera: giant rats *Kunsia*, swamp rats *Scapteromys*, Andean rats *Lenoxus*, and *Brucepattersonius*), *Calomys*, and *Lophuromys* showed high evolution rates but unremarkable disparities (Table 6; Fig. 5e–h).

The consistent results observed across GM/LM/size/shape datasets reflect the fact that, except for LM shape disparity/evolution rate versus LM size disparity/evolution rate contrasts, all other variables were correlated. The correlation between size and shape evolution/disparity can be explained by shared allometric relationships, whereby cranial shape is highly dependent on size leading similar sized crania to have similar shapes. However, this correlation can also occur if different subclades within a focal clade undergo decoupled increases size and shape evolution rates (Adams et al. 2009).

Likewise, alternative measures of diversification were strongly correlated: diversification rates with net diversity ($p < 0.0001$, $R^2 = 0.689$; Table 6; Fig. 6j) and rates of morphological evolution with disparity (all p values < 0.0003 , $R^2 = 0.332–0.883$; Table 6; Fig. 6e–h). The fact that clade age was not correlated with disparity (Table 6; Fig. 6a–d) or diversity (Table 6; Fig. 6i) implies that the variation in origination times of sampled clades (from 1.5 to 5 mya) did not have a major effect on the observed patterns of association between diversity and disparity/evolutionary rate. This decoupling may also indicate that 4.5 mya is not sufficient time to accumulate significant variation in diversity and disparity/evolutionary rate in muroids, however, there

was some evidence that clades with exceptional disparity were relatively old (e.g. Murinae clade X, Murinae clade XI, Sigmodontinae clade IX, and Sigmodontinae clade XII) and that recently evolved clades had the lowest disparities (e.g. *Dendromys* and *Lophuromys*).

Causes of Decoupled Diversity and Disparity/Evolutionary Rate

Despite using the GM approach, which is especially successful at detecting relatively low levels of morphological variation between morphologically similar species (Zelditch et al. 2004), we found no correlation between disparity/evolutionary rate and diversity. Moreover, this result is based on perhaps the most important morphological index of ecology and niche in mammals, the cranial organ system, which houses most sensory and masticatory structures and is among the most variable structures in muroids (Nowak 1999), and therefore, the most likely to show a pattern if it does exist than other morphological traits. For example, cranial size and shape are more useful indicators of general feeding ecology than body size and shape because they more directly measure gape size and feeding adaptations.

It is unlikely that the decoupling of diversity and disparity/evolutionary rate is a consequence of methodological artifacts since the pattern was robust to the use of multiple indices of morphology and clades extracted from different time periods. Furthermore, the range of variation in disparity/evolutionary rate and diversity was sufficient enough to detect correlations between disparity/evolutionary rate and other variables (e.g. GM and LM disparity vs. evolution rate; GM vs. LM size and shape variables) and between diversity and other variables (e.g. diversification rate vs. net diversity).

The decoupling of diversity and disparity/evolutionary rate is perhaps less surprising in more recent than older clades because many recent clades have species with very similar external morphologies (e.g. *Rattus*, Rowe et al. 2011) with morphologically cryptic species being increasingly described solely based on molecular data (e.g. *Niviventer*, He and Jiang 2013). This explanation might account for some of the pattern, since clades such as Murinae clade VIII (includes both *Rattus* and *Niviventer*) have high diversity/diversification rate and low disparity/evolution rate (Tables 2, 5; Fig. 5). However, it is unlikely to explain the overall pattern since similar results were observed in clades extracted at different time intervals. Furthermore, the relatively recent genus, with known morphologically cryptic species, *Calomys* (e.g. González Ittig et al. 2002), had high GM and LM shape evolution rates but low diversity/diversification rates (Tables 2, 5; Fig. 5e, g); opposite of the expected pattern if the prevalence of

cryptic species explains the lack of relationship between diversity and disparity/evolutionary rate.

Variation in both diversity and disparity/evolutionary rate could be explained by other factors such as ecological opportunity mediated by biogeographic transitions. There is some evidence for this presented by Schenk et al. (2013) and Alhajeri et al. (2016), where the primary colonization of South America, Sahul, and Southeast Asia were associated with increased phylogenetic and phenotypic diversification in muroid rodents, although this pattern cannot be generalized to other primary and secondary colonization. Other unexamined triggers of ecological opportunity may also explain patterns of diversity and disparity/evolutionary rate in muroids such as mass extinctions of protagonists and the evolution of key innovations (Simpson 1953; Schluter 2000; Grant and Grant 2008). Speciation/diversification rates in muroids may also be associated with directional ecomorphological adaptation (rather than unspecific morphological divergence).

The predictions of Schluter's (2000) model of ecological adaptive radiation assumes that increased diversification rates are precipitated by reduced niche overlap between the diversifying lineages and closely related, sympatric groups, leading to adaptive divergence as recently diverged species occupy new ecological niches (Simpson 1944; Freckleton and Harvey 2006). Such a pattern is not observed in muroids; rather all families were highly overlapping in morphospace in both size (Fig. 3) and shape (Fig. 4); a situation that could lead to clades constraining each other's diversification rates. Nor is there evidence for the prediction among younger clades. However, the fact that the families with the most divergent morphospace occupation (nesomyids, dipodids, and spalacids; Figs. 3, 4) are among the least diverse may indicate that muroid diversification occurs within a shared region of morphospace, a pattern that has been documented in other taxa (e.g. birds, Ricklefs 2005; plethadon salamanders; Adams et al. 2009).

Other potential causes of increased diversification rates in clades that are not investigated in the present study include clade allopatry relative to others, which in theory could allow lineages sufficient freedom to diversify into adaptive zones without being crowded by close competitors; a similar explanation to the biogeographically induced ecological opportunity model tested by Schenk et al. (2013). However, it is unlikely, that allopatry enhances diversification and morphological evolution rates in muroids considering that the allopatric nesomyid clades in Madagascar are unremarkable in both indices whereas Murinae clades (Southeast Asian clade VIII and Sahulian clade XI) have among the highest diversification rates while being sympatric with other clades in that region.

Conclusion

Muroid diversity does not appear to be correlated with disparity/evolutionary rate, a result that is robust to variations in morphological datasets and clade designations. This result contradicts most well-known evolutionary theories that predict a correlation such as the punctuated equilibrium and the ecological adaptive radiation models. However, other recent empirical studies conducted on other taxa, similarly show a decoupling of diversity and disparity/evolutionary rate which indicates that increased diversification is not always accompanied by increased morphological divergence and vice versa.

We also found that phylogenetic and non-phylogenetic estimates of diversity and disparity/evolutionary rate are highly correlated, and consequently led to similar results. Clade age was not significantly correlated with diversity and disparity/evolutionary rate which suggests that diversity cannot be explained by clade age. Finally, the great extent of the overlap in morphospace in myodont families suggests an overall similar cranial morphology and that muroid diversification occurs within a shared region of morphospace.

Acknowledgements We thank all museum curators and collection managers for access to their collections: United States National Museum of Natural History (Kristofer Helgen, Darrin Lunde, Helen Kafka, and Michael D. Carleton); Field Museum of Natural History (Lawrence R. Heaney, William Stanley, John Phelps, Julian C. Kerbis-Peterhans, and Bruce D. Patterson); Museum of Vertebrate Zoology, Berkeley (James L. Patton and Chris Conroy); University of Florida Museum of Natural History (Candace McCaffery and David Reed); American Museum of Natural History (Darrin Lunde and Eileen Westwig); Laboratorio de Citogenética Mamíferos, Universidad de Chile (Angel Spotorno and Laura Walker); and Oklahoma Museum of Natural History (Michael Mares, Janet K. Braun, Hayley Lanier, and Brandi S. Coyner). John Schenk helped with research design. Earlier versions of the manuscript benefited from comments by Gregory Erickson, Joseph Travis, Thomas Miller, and William Parker. The final version of this manuscript was improved by comments from two anonymous reviewers.

Funding Financial support for this work was provided by a doctoral dissertation fellowship from Kuwait University to BHA (to the Florida State University) and a Grant from the National Science Foundation to SJS (DEB-0841447).

Compliance with Ethical Standards

Conflict of interest The authors declare that they have no conflict of interest.

References

- Adams, D. C., Berns, C. M., Kozak, K. H., & Wiens, J. J. (2009). Are rates of species diversification correlated with rates of morphological evolution? *Proceedings of the Royal Society B: Biological Sciences*, 276(2729), 2738. <https://doi.org/10.1098/rspb.2009.0543>.
- Adams, D. C., & Otárola-Castillo, E. (2013). Geomorph: An R package for the collection and analysis of geometric morphometric shape data. *Methods in Ecology and Evolution*, 4(4), 393–399. <https://doi.org/10.1111/2041-210X.12035>.
- Akaike, H. (1974). A new look at statistical model identification. *IEEE Transactions on Automatic Control*, 19, 716–723.
- Alhajeri, B. H. (2014). *Adaptation, diversification, and desert ecology of the most diverse order of mammals (Mammalia, Rodentia)*. Tallahassee, FL: Department of Biological Science, Florida State University.
- Alhajeri, B. H., Schenk, J. J., & Stepan, S. J. (2016). Ecomorphological diversification following continental colonization in muroid rodents (Rodentia: Muroidea). *Biological Journal of the Linnean Society*, 117(3), 463–481. <https://doi.org/10.1111/bij.12695>.
- Alhajeri, B. H., & Stepan, S. J. (2018). Ecological and ecomorphological specialization are not associated with diversification rates in muroid rodents (Rodentia: Muroidea). *Evolutionary Biology*. <https://doi.org/10.1007/s11692-018-9449-8>.
- Álvarez, A., & Perez, S. I. (2013). Two- versus three-dimensional morphometric approaches in macroevolution: Insight from the mandible of caviomorph rodents. *Evolutionary Biology*, 40(1), 150–157. <https://doi.org/10.1007/s11692-012-9194-3>.
- Blankers, T., Adams, D. C., & Wiens, J. J. (2012). Ecological radiation with limited morphological diversification in salamanders. *Journal of Evolutionary Biology*, 25(4), 188–203. <https://doi.org/10.1111/j.1420-9101.2012.02458.x>.
- Cardini, A. (2016). Lost in the other half: Improving accuracy in geometric morphometric analyses of one side of bilaterally symmetric structures. *Systematic Biology*, 65(6), 1096–1106.
- Cheverud, J. M. (1995). Morphological integration in the saddle-back tamarin (*Saguinus fuscicollis*) Cranium. *The American Naturalist*, 145(1), 63–89.
- Cheverud, J. M. (1995). Morphological integration in the saddle-back tamarin (*Saguinus fuscicollis*) Cranium. *The American Naturalist*, 145(1), 63–89. Retrieved from <http://www.jstor.org/stable/2463147>.
- Claude, J. (2008). *Morphometrics with R*. New York: Springer.
- Clavel, J. (2014). mvMORPH: Multivariate comparative tools for fitting evolutionary models to morphometric data. R package version 1.0.1. Retrieved from <http://cran.r-project.org/web/packages/mvMORPH/index.html>.
- Fabre, P.-H., Hautier, L., Dimitrov, D., & Douzery, E. (2012). A glimpse on the pattern of rodent diversification: A phylogenetic approach. *BMC Evolutionary Biology*, 12(1), 1–19. <https://doi.org/10.1186/1471-2148-12-88>.
- Foote, M. (1993). Contributions of individual taxa to overall morphological disparity. *Paleobiology*, 19(4), 403–419. Retrieved from <http://paleobiol.geoscienceworld.org/content/19/4/403.short>.
- Freckleton, R. P., & Harvey, P. H. (2006). The evolution of morphological diversity. *PLoS Biology*, 4(11), 2104–2111. Retrieved from <http://europepmc.org/abstract/MED/17090217>.
- Funk, D. J., Nosil, P., & Etges, W. J. (2006). Ecological divergence exhibits consistently positive associations with reproductive isolation across disparate taxa. *Proceedings of the National Academy of Sciences of the United States of America*, 103(9), 3209–3213. <https://doi.org/10.1073/pnas.0508653103>.
- González Ittig, R. E., Chiappero, M. B., Blanco, A., Provencal, C., & Gardenal, C. N. (2002). Accurate identification of three cryptic species of rodents of the genus *Calomys* using RAPD-PCR and mitDNA RFLP markers. *Biochemical Systematics and Ecology*, 30(5), 425–432. [https://doi.org/10.1016/S0305-1978\(01\)00107-7](https://doi.org/10.1016/S0305-1978(01)00107-7).
- Gonzalez-Voyer, A., Padial, J. M., Castroviejo-Fisher, S., De La Riva, I., & Vilà, C. (2011). Correlates of species richness in the largest Neotropical amphibian radiation. *Journal of*

- Evolutionary Biology*, 24(5), 931–942. <https://doi.org/10.1111/j.1420-9101.2011.02243.x>.
- Gould, S. J., & Eldredge, N. (1977). Punctuated equilibria; the tempo and mode of evolution reconsidered. *Paleobiology*, 3(2), 115–151. Retrieved from <http://paleobiol.geoscienceworld.org/content/3/2/115.short>.
- Grant, P. R., & Grant, B. R. (2008). *How and why species multiply? The radiation of Darwin's Finches*. New Jersey: Princeton University Press.
- Harmon, L. J., Schulte, J. A., Larson, A., & Losos, J. B. (2003). Tempo and mode of evolutionary radiation in iguanian lizards. *Science*, 301(5635), 961–964. <https://doi.org/10.1126/science.1084786>.
- Harmon, L. J., Weir, J. T., Brock, C. D., Glor, R. E., & Challenger, W. (2008). GEIGER: Investigating evolutionary radiations. *Bioinformatics*, 24(1), 129–131. <https://doi.org/10.1093/bioinformatics/btm538>.
- He, K., & Jiang, X.-L. (2013). Mitochondrial phylogeny reveals cryptic genetic diversity in the genus *Niviventer* (Rodentia, Muroidea). Mitochondrial DNA. <https://doi.org/10.3109/19401736.2013.823167>.
- Hopkins, M. J. (2013). Decoupling of taxonomic diversity and morphological disparity during decline of the Cambrian trilobite family Pterocerphaliidae. *Journal of Evolutionary Biology*, 26(8), 1665–1676. <https://doi.org/10.1111/jeb.12164>.
- Magallón, S., & Sanderson, M. J. (2001). Absolute diversification rates in angiosperm clades. *Evolution*, 55(9), 1762–1780.
- Marroig, G., & Cheverud, J. M. (2001). A comparison of phenotypic variation and covariation patterns and the role of phylogeny, ecology, and ontogeny during cranial evolution of New World monkeys. *Evolution*, 55(12), 2576–2600.
- Martins, E. P., & Hansen, T. F. (1997). Phylogenies and the comparative method: A general approach to incorporating phylogenetic information into the analysis of interspecific data. *The American Naturalist*, 149(4), 646–667.
- Musser, G. G., & Carleton, M. D. (2005). Superfamily Muroidea. In D. E. Wilson & D. M. Reeder (Eds.), *Mammal species of the world* (pp. 894–1531, 3rd ed.). Baltimore: The Johns Hopkins University Press.
- Nowak, R. M. (1999). *Walker's mammals of the world* (Vols. 1 and 2, 6th ed.). Baltimore: John Hopkins University Press.
- O'Meara, B. C., Ané, C., Sanderson, M. J., & Wainwright, P. C. (2006). Testing for different rates of continuous trait evolution using likelihood. *Evolution*, 60(5), 922–933. <https://doi.org/10.1111/j.0014-3820.2006.tb01171.x>.
- Orme, D., Freckleton, R., Thomas, G., Petzoldt, T., Fritz, S., Isaac, N., & Pearse, W. (2013). CAPER: Comparative analyses of phylogenetics and evolution in R. <https://cran.r-project.org/package=caper>.
- Paradis, E., Claude, J., & Strimmer, K. (2004). APE: Analyses of phylogenetics and evolution in R language. *Bioinformatics*, 20(2), 289–290. <https://doi.org/10.1093/bioinformatics/btg412>.
- Patterson, B., & Pascual, R. (1968). Evolution of mammals on southern continents. V. The fossil mammal fauna of South America. *The Quarterly Review of Biology*, 43(4), 409–451. Retrieved from <http://www.jstor.org/stable/2819014>.
- Purvis, A. (2004). Evolution: How do characters evolve? *Nature*. <https://doi.org/10.1038/nature03092>.
- R Development Core Team. (2017). R: A language and environment for statistical computing. <http://www.r-project.org/>.
- Rabosky, D. L. (2009a). Ecological limits on clade diversification in higher taxa. *American Naturalist*, 173, 662–674.
- Rabosky, D. L. (2009b). Ecological limits and diversification rate: Alternative paradigms to explain the variation in species richness among clades and regions. *Ecology Letters*, 12(8), 735–743. <https://doi.org/10.1111/j.1461-0248.2009.01333.x>.
- Rabosky, D. L., & Adams, D. C. (2012). Rates of morphological evolution are correlated with species richness in salamanders. *Evolution*, 66(6), 1807–1818. <https://doi.org/10.1111/j.1558-5646.2011.01557.x>.
- Rabosky, D. L., Santini, F., Eastman, J., Smith, S. A., Sidlauskas, B., Chang, J., & Alfaro, M. E. (2013). Rates of speciation and morphological evolution are correlated across the largest vertebrate radiation. *Nature Communications*, 4, 1958. <https://doi.org/10.1038/ncomms2958>.
- Ricklefs, R. E. (2004). Cladogenesis and morphological diversification in passerine birds. *Nature*, 430(6997), 338–341. <https://doi.org/10.1038/nature02700>.
- Ricklefs, R. E. (2005). Small clades at the periphery of passerine morphological space. *American Naturalist*, 165, 651–659.
- Ricklefs, R. E. (2006). Time, species, and the generation of trait variance in clades. *Systematic Biology*, 55(1), 151–159. <https://doi.org/10.1080/10635150500431205>.
- Robertson, R. A., & Shadle, A. R. (1954). Osteologic criteria of age in beavers. *Journal of Mammalogy*, 35(2), 197–203. Retrieved from <http://www.jstor.org/stable/1376033>.
- Rohlf, F. J., & Slice, D. (1990). Extensions of the procrustes method for the optimal superimposition of landmarks. *Systematic Biology*, 39(1), 40–59. <https://doi.org/10.2307/2992207>.
- Rowe, K. C., Aplin, K. P., Baverstock, P. R., & Moritz, C. (2011). Recent and rapid speciation with limited morphological disparity in the Genus *Rattus*. *Systematic Biology*, 60(2), 188–203. <https://doi.org/10.1093/sysbio/syq092>.
- Rundell, R. J., & Price, T. D. (2009). Adaptive radiation, nonadaptive radiation, ecological speciation and nonecological speciation. *Trends in Ecology & Evolution*, 24(7), 394–399. <https://doi.org/10.1016/j.tree.2009.02.007>.
- Schenk, J. J., Rowe, K. C., & Stepan, S. J. (2013). Ecological opportunity and incumbency in the diversification of repeated continental colonizations by muroid rodents. *Systematic Biology*, 62(6), 837–864.
- Schluter, D. (2000). *The ecology of adaptive radiation*. Oxford: Oxford University Press.
- Simpson, G. G. (1944). *Tempo and mode in evolution*. New York: Columbia University Press.
- Simpson, G. G. (1953). *The major features of evolution*. New York: Columbia University Press.
- Slater, G. J., Price, S., Santini, F., & Alfaro, M. E. (2010). Diversity versus disparity and the radiation of modern cetaceans. *Proceedings of the Royal Society B: Biological Sciences*, 277, 3097–3104. <https://doi.org/10.1098/rspb.2010.0408>.
- Slater, G. J., Price, S. A., Santini, F., & Alfaro, M. E. (2010). Diversity versus disparity and the radiation of modern cetaceans. *Proceedings of the Royal Society B: Biological Sciences*. <https://doi.org/10.1098/rspb.2010.0408>.
- Slice, D. E. (2009). *Morpheus et al. (alpha)*. Tallahassee, FL: Department of Scientific Computing, Florida State University.
- Sneath, P. H. A., & Sokal, R. R. (1973). *Numerical taxonomy*. San Francisco: Freeman.
- Stacklies, W., Redestig, H., Scholz, M., Walther, D., & Selbig, J. (2007). pcaMethods—A bioconductor package providing PCA methods for incomplete data. *Bioinformatics*, 23(9), 1164–1167. <https://doi.org/10.1093/bioinformatics/btm069>.
- Stepan, S. J. (1997). Phylogenetic analysis of phenotypic covariance structure. I. Contrasting results from matrix correlation and common principal component analysis. *Evolution*, 51(2), 571–586. <https://doi.org/10.2307/2411129>.
- Stepan, S. J., & Schenk, J. J. (2017). Muroid rodent phylogenetics: 900-species tree reveals increasing diversification rates. *PLoS ONE*, 12(8), 1–31. <https://doi.org/10.1371/journal.pone.0183070>.

- Wilson, L. A. B., & Sánchez-Villagra, M. R. (2010). Diversity trends and their ontogenetic basis: An exploration of allometric disparity in rodents. *Proceedings of the Royal Society B: Biological Sciences*, *B277*, 1227–1234. <https://doi.org/10.1098/rspb.2009.1958>.
- Zelditch, M. L., Swiderski, D. L., Sheets, H. D., & Fink, W. L. (2004). *Geometric morphometrics for biologists: A primer*. London: Elsevier Academic Press.